lubricants

MDPI

Article

Study on the Friction Characteristics and Fatigue Life of Carbonitriding-Treated Needle Bearings

Yong Chen [1,*], Xiangrun Pu [2], Lijie Hao [2], Guangxin Li [2] and Li Luo [1]

[1] State Key Laboratory of Featured Metal Materials and Life-Cycle Safety for Composite Structures, Guangxi University, Nanning 530004, China; luoli178050512@163.com
[2] Tianjin Key Laboratory of Power Transmission and Safety Technology for New Energy Vehicles, School of Mechanical Engineering, Hebei University of Technology, Tianjin 300130, China; a17854190711@163.com (X.P.); jiejiehao2021@163.com (L.H.); ligx1229@163.com (G.L.)
* Correspondence: chenyong1585811@163.com

Abstract: Being a key component of the transmission system, the needle bearing's performance and service life affects the overall service life of mechanical equipment. This study takes needle bearings composed of AISI 52100 steel as the research object and studies the effect of carbonitriding surface strengthening treatment on the bearing friction, wear, and fatigue life. The carbon and nitrogen co-infiltration surface-strengthening method was employed to prepare cylindrical and disc samples. The surface hardness, residual austenite content, microscopic morphology and organization composition, coefficient of friction, and wear scar were studied to analyze the effect on the wear performance of the material. The bearing fatigue wear comparison test was conducted on a test bench to compare the actual fatigue life and surface damage of the needle bearing through conventional martensitic quenching heat treatment and carbonitriding treatment. The results demonstrate that the carbonitriding strengthening method enhances the toughness of the material while improving its surface hardness. It also improves the wear resistance of the needle roller bearings, and the fatigue life of the bearings is significantly improved. In conclusion, carbon and nitrogen co-infiltration treatment is a strengthening method that effectively extends the service life of needle roller bearings, indicating its high practical value.

Keywords: carbonitriding treatment; needle bearing; friction characteristics; fatigue life; experimentation; simulation

Citation: Chen, Y.; Pu, X.; Hao, L.; Li, G.; Luo, L. Study on the Friction Characteristics and Fatigue Life of Carbonitriding-Treated Needle Bearings. *Lubricants* **2024**, *12*, 234. https://doi.org/10.3390/lubricants12070234

Received: 26 April 2024
Revised: 4 June 2024
Accepted: 21 June 2024
Published: 24 June 2024

1. Introduction

As an important type of mechanical component, needle bearings have the function of speed and torque transmission. In the working process, the needle rollers repeatedly make contact with the shaft and the outer bore. The contact surface is subjected to high alternating stress, which generates a significant amount of heat due to mutual friction. This leads to a reduction in hardness and plastic deformation, thereby reducing the service life of the material [1]. The chosen rolling bearings must not only display the required strength, but must also have excellent fatigue resistance [2].

Contact fatigue wear is one of the most prevalent forms of friction failure in roller bearings. A considerable number of scholars have conducted research into the contact fatigue and friction characteristics of bearings [3–5]. Wang et al. [6] established a fatigue damage accumulation model to analyze the subsurface crack evolution and fatigue life of rolling contact fatigue. Morales-Espejel et al. [7] investigated the effect of roughness on contact bearings. Smolnicki et al. [8] adjusted the bearing finite element model's mesh size to study and analyze load distribution. Lostado et al. [9] carried out a stress analysis of a bearing using a numerical simulation model and compared the theoretical model with the results of contact sensor measurements. Kania et al. [10] studied the variation rules of the contact stresses and strains in various bearing parts. Bakolas et al. [11] proposed a

method for the estimation of the frictional energy loss of a specific bearing type on a global scale. Ilie [12] conducted a study to analyze the diffusion and mass transfer mechanisms in a friction couple comprising steel and bronze. Previous studies have pointed out that the failure due to contact fatigue mainly occurs on the surface or in the subsurface. A mere improvement in the manufacturing precision or enhancement in the material composition cannot adequately increase the surface properties of the material. These measurements need to be combined with surface strengthening treatment technology.

Regarding the AISI 52100 bearing's carbonitriding process, the research analysis is mainly based on the test results, focusing on the influence of the furnace temperature, quenching temperature, carbon potential, and other factors on the organizational characteristics. Huan et al. [13] explored the improvement of the properties of AISI 52100 steel through two strengthening treatments, namely pre-carburizing + quenching and tempering versus, carbonitriding + quenching and temperature. The results showed that the latter could effectively reduce the friction coefficient and wear rate of AISI 52100 steel. Wan et al. [14] investigated the effect of laser impact shot peening and vacuum carburizing on the strength and plasticity of a 20CrMn2Mo alloy. The results showed that the yield and tensile strength of the treated material were improved. Rajan et al. [15] concluded that an AISI 52100 ball bearing's reliability was effectively improved after carbonizing. Liu et al. [16] conducted a detailed analysis of the black structure produced by carbonitriding the inner and outer rings of AISI 52100 bearings. Zhao et al. [17] investigated the bearing inner and outer rings of the quenching structure and the surface hardness under carbonitriding pretreatment. Karamis et al.'s [18] analysis showed that carbon–nitrogen strengthening increased the AISI 1020 mild steel's surface hardness by two times; its inherent toughness was not reduced, and the tribological properties were improved significantly. Kanchanomai et al. [19] analyzed the carbonitriding alloy steel's fatigue performance via residual compressive stress, concluding that the fatigue life of the carbonitriding steel was approximately five times that of a sample without carbonitriding treatment. Jiang et al. [20] used gas carbonitriding technology to strengthen the surface of martensitic bearing steel, significantly improving the residual compressive stress and austenite content of the sample. Co-infiltration heat treatment with carbon and nitrogen can effectively improve the material properties. Further research is required to know the effect of this process on the anti-wear performance and fatigue life of needle bearings.

In this study, research was conducted on carbonitride-strengthened needle bearings. The effect of the carbonitriding heat treatment on their surface friction and wear performance and fatigue life is discussed. Conventional martensitic quenching and tempering treatment and carbonitriding surface strengthening treatment were carried out on the bearing material AISI 52100 to produce test specimens and test bearings, respectively. The surface hardness, residual austenite content, microscopic morphology and organization composition, coefficient of friction, and wear scar were used to investigate the effectiveness of the conventional heat treatment. The fatigue life test was carried out on a fatigue test rig. A comparison of the fatigue life results and surface failure status of conventionally heat–treated needle bearings with those of carbonitriding-treated needle bearings is presented.

2. Materials

2.1. Preparation of Test Disc Samples

Before carrying out the friction wear and fatigue life tests, AISI 52100 steel was selected as the basic material to prepare the required specimens and needle bearings. The chemical composition of AISI 52100 steel is shown in Table 1.

Table 1. Chemical composition of AISI 52100 bearing steel materials.

Element	C	Si	Mn	P	S	Cr	Ti	H	O
Mass fraction (%)	0.98	0.22	0.33	0.010	0.003	1.48	0.0025	0.0001	0.0006

AISI 52100 bearing steel is an American standard high-strength alloy structural steel. The reference standard is ASTM A 29/A 29M-04 [21]. The corresponding ISO grade of this steel is 100Cr6, and the corresponding Chinese standard steel type is GCr15. The reference standard is ISO 683-17: 2014 [22]. These are designated as AISI 52100.

Since the contact form in needle bearings is primarily linear, tests were conducted with a disc that had a diameter of 24 mm and a thickness of 7.9 mm, as well as a cylinder with a diameter of 6 mm and a length of 8 mm. The test specimens are shown in Figure 1.

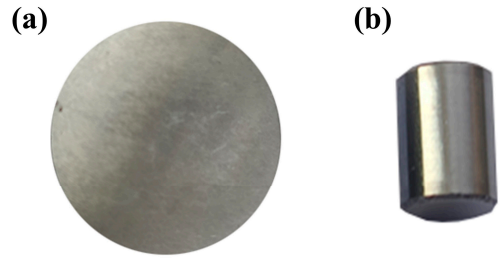

Figure 1. Disc and cylindrical specimens for testing: (**a**) the surface of the test disc (view); (**b**) the cylindrical specimen.

2.2. Carbonitriding Process

A controlled-atmosphere multi-purpose gas chamber furnace heat treatment production line was utilized for the corresponding carbon and nitrogen co-infiltration process. The furnace atmosphere consisted of carbon potential (CP) = 0.9~1.2%, CO_2 = 0.2~0.4%, NH_3 = 0.1~0.5%. After the product's quenching out of the furnace, it was placed in a vacuum cleaning machine before tempering.

The following chemical reactions occur during carbonitriding:

$$CH_4 + NH_3 \rightarrow HCN + 3H_2 \quad (1)$$

$$CO + NH_3 \rightarrow HCN + H_2O \quad (2)$$

$$2HCN \rightarrow H_2 + 2[C] + 2[N] \quad (3)$$

The depth of the carbonitride layer on the AISI 52100 bearing steel after carbonitriding treatment was 0.4–0.7 mm. The carbon concentration of the carbonitriding bearing surfaces was approximately 1.2%, and the carbon concentration of ordinary bearing steel is approximately 0.9–0.95%. After the carbonitriding treatment of the bearing steel, the infiltration layer's organization consisted of a small quantity of nitrogen and carbon compounds, nitrogenous martensite, residual austenite, and a small quantity of carbides.

2.3. Lubrication Conditions

To ensure the accuracy and consistency of the test results, the same lubricant was used for the wear tests and life tests. Table 2 shows the parameters of the utilized lubricants. The same amount of lubricant was added to each group before testing.

Table 2. Lubricant parameters.

Parameters	L-HM 32
Density at 20 °C ($kg \cdot m^{-3}$)	854.0
Dynamic viscosity at 40 °C ($mm^2 \cdot s^{-1}$)	32.11
Dynamic viscosity at 100 °C ($mm^2 \cdot s^{-1}$)	5.580
Viscosity index	112

2.4. Needle Bearing Models

In this study, the needle bearing K28 × 33 × 19 composed of AISI 52100 bearing steel, was selected as the main research object. The physical object is shown in Figure 2a,b, the

geometrical parameters are shown in Table 3, and its three-dimensional model is shown in Figure 2c.

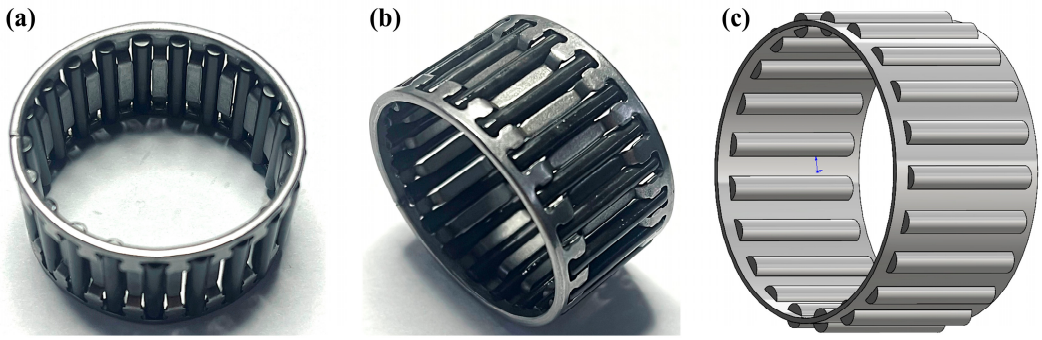

Figure 2. Needle bearing K28 × 33 × 19 (**a**,**b**) needle bearing object; (**c**) needle bearing 3D model.

Table 3. The parameters of needle bearing K28 × 33 × 19.

Parameter	Value
Dimension (mm)	28 × 33 × 19
Needle diameter (mm)	2.5
Needle roller length (mm)	15.8
Number of rolling bodies (Pcs)	21
Needle roller tolerance grade	G2
Pitch circle diameter (mm)	30.5
Ultimate RPM (rpm)	16,000
Rated dynamic load (kN)	19.6
Rated static load (kN)	32.4

3. Methods

3.1. Line Contact Friction Test

The Schwing-Reib-Verschleiss-5 (SRV-5) tester, manufactured by the Optimol Instruments Prueftechnik GmbH (München, Germany), is a physical property testing instrument used for friction and wear testing in the physical field. The SRV-5 test setup is shown in Figure 3a and the motion shape of the specimen under test is shown in Figure 3b. During the test, the lower specimen (disc) was held in place, while the upper specimen (cylinder) was subjected to reciprocating frictional movement. Prior to the test, the lubricant was injected through a burette into the contact area between the upper and lower specimens. The load was applied vertically to the disc through a transducer.

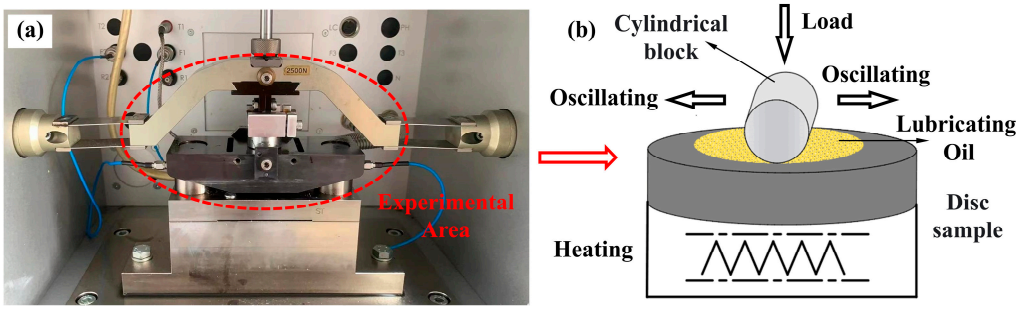

Figure 3. SRV-5 friction and wear test rig: (**a**) SRV-5 test equipment; (**b**) test motion principle.

Taking the automatic transmission bearings as the research object, the maximum input torque was usually between 250 Nm and 350 Nm, and the contact stress was between 1000 and 2500 MPa. Taking the working conditions of the bearing test as the reference, in combination with the D7421-11 [23] of the American Society for Testing and Materials

(ASTM), the test loads were set at 100 N, 200 N, and 300 N. The specific test parameters are shown in Table 4 [24].

Table 4. SRV friction and wear test parameters.

Test Parameter	Line Contact Experiments
Load (N)	100/200/300
Experimental period (s)	3600
Temperature (°C)	80
Frequency (Hz)	50
Sliding velocity (m/s)	0.1
Oil volume (mL)	0.3

3.2. Surface Inspection of Test Samples

The subject of the carbonitriding needle bearing surface inspection project, which was the subject of this study, involved the following equipment:

(1) The HMV-G series micro-Vickers hardness tester produced by QATM GmbH (Mammelzen, Germany), was used for the surface hardness measurement of the samples;

(2) An AreX-L diffraction analyzer (X-ray diffractometer, XRD) from GND S.R.L. (Agrate Conturbia, Italy) was employed to investigate the variations in the residual austenite content. During the measurements, Mo radiation and a 1 mm collimator were applied to detect the magnitude of the diffraction angle and the intensity of the diffraction peaks at (200) α, (211) α, (200) γ, (220) γ, and (311) γ, respectively;

(3) The surface was analyzed using a scanning electron microscope (SEM) manufactured by JEOL K.K. (Tokyo, Japan). An energy spectrometer (Energy-Dispersive Spectrometer, EDS) from Oxford Instruments PLC (Oxfordshire, England) were used to observe the morphology and composition of the surface of each sample;

(4) A SURFCOM NEX 001SD-12 surface roughness measurement instrument manufactured by Tokyo Seimitsu CO., LTD (Tokyo, Japan) was employed to assess the surface roughness of the disc samples. The three-dimensional morphology and roughness were analyzed using white light interferometry, provided by Bruker Nano Surfaces (Beijing, China).

3.3. Fatigue Life Simulation

The needle and rotating shaft contact of needle bearings can be considered as line contact and calculated using Hertz contact theory. The two-cylinder contact was simplified as an equivalent cylinder and infinite-length plane contact, and the empirical formula proposed by Palmgren was used to calculate the elastic deformation convergence δ:

$$\delta = 3.81\left(\frac{1-\nu_1^2}{\pi E_1}+\frac{1-\nu_2^2}{\pi E_2}\right)^{0.9}\frac{Q^{0.9}}{l^{0.8}} \tag{4}$$

where Q is the rolling load, and l is the rolling body length. For steel bearings, $\nu_1 = \nu_2 = 0.3$, $E_1 = E_2 = 2.06 \times 10^5$ N/mm^2. For rolling bearings, the rated life can be calculated using Equation (5):

$$L_{10} = \left(\frac{C}{P}\right)^{\varepsilon} \tag{5}$$

where L_{10} is the rated life in 10^6 revolutions, P is the equivalent dynamic load, and C is the dynamic load rating of the bearing. When the outer ring is stationary and the inner ring is rotating, the rated life of the bearing is calculated in terms of the number of revolutions and the continuous load in one direction that it can withstand. C can be obtained from Equation (6).

$$C = b_m f_c (il\cos\alpha)^{\frac{7}{9}} Z^{\frac{3}{4}} D_w^{\frac{29}{27}} \tag{6}$$

In the formula, b_m is the material correction factor; for needle bearings, it usually takes a value of 1. f_c is the rated basic life calculation coefficient of the bearing, which is usually closely related to the bearing's geometric parameters. i refers to the rolling bearing with i rows of rolling elements. a refers to the nominal contact angle of the bearing. Z refers to the number of rolling elements. D_w is the diameter of the needle rollers.

The equivalent dynamic load P of a bearing describes the value of the load that the bearing can support while operating. The equivalent dynamic load is defined as a preset load of constant magnitude and direction, under which the fatigue service life of a bearing is equivalent to its service life under an actual load. In the case of needle bearings subjected to radial loads, the equivalent dynamic load can be determined using Equation (7).

$$P = xF_r + yF_a \tag{7}$$

F_r represents the radial load, while F_a is the axial load. It can be demonstrated that a needle bearing is capable of resisting only radial forces and is, therefore, unable to withstand axial forces. Consequently, the values of x and y are both equal to 1. Moreover, x is assigned a numeric value of 1, and y is assigned a value of 0. During the calculation process, the fatigue life of needle bearings is commonly expressed in terms of the total number of hours for which the bearing has been in operation. If the rotational speed of the bearing is known, the correction factor in Equation (5) is adjusted to read as follows.

$$L_h = \frac{10^6}{60n}\left(\frac{C}{P}\right)^{\varepsilon} \tag{8}$$

where L_h is the bearing life calculated via the number of working hours, and n is the rotational speed of the bearing, where the unit is r/min.

To ascertain the impact of the carbonitriding treatment process on the lifespan of the needle bearings, the Romax DT 2023.1 bearing professional analysis software was used. This enabled the set-up for construction of a needle bearing test bench model, which was then used to compare and analyze the lifespans of the needle bearings before and after the carbonitriding treatment. The three-dimensional model of the axle system of the needle bearing test bench and the physical figure are presented in Figure 4.

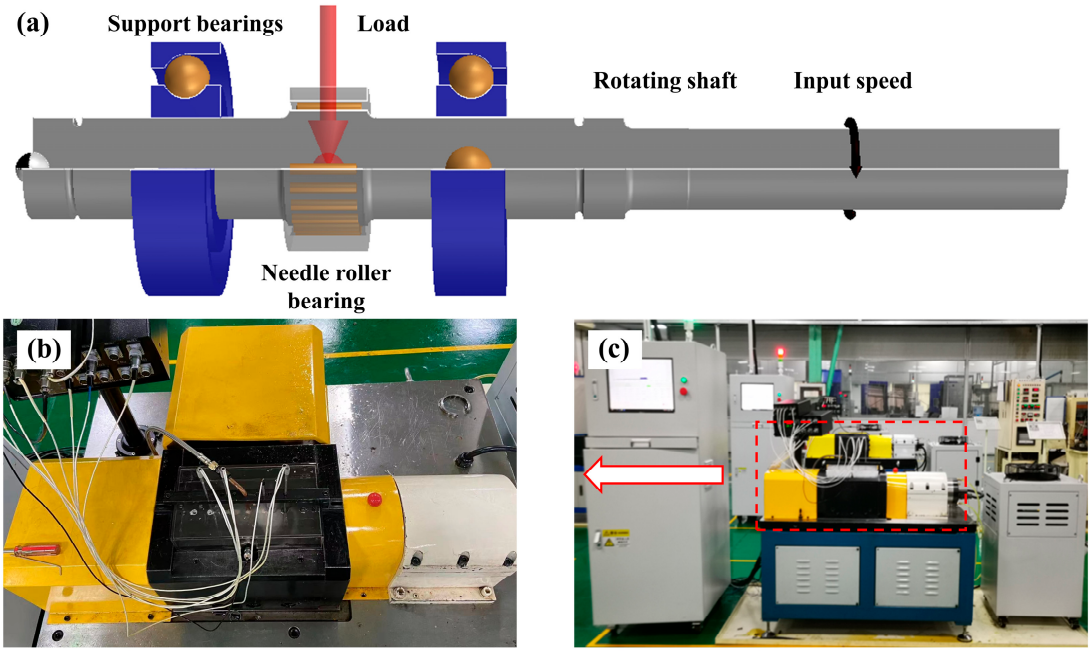

Figure 4. Needle bearing life simulation and experiment: (**a**) needle bearing test rig model; (**b**,**c**) schematic diagram of needle bearing test rig.

3.4. Fatigue Life Test

The needle bearing life test adopted a radial load of 2~4 tons in a type II testing machine. The equipment was programmed to operate automatically in accordance with the pre-set test load, speed, and running time, as well as other main parameters. It employed a vibration and temperature over-run control mode, and utilized the hydraulic step-by-step loading method to subject the bearing to the test load in stages.

A number of sets of needle bearings were prepared for the conventional heat treatment and carbonitriding treatment. These tests utilize two test conditions, normal load and high load, with each condition being prepared with two sets of conventional heat treatment and two sets of carbonitriding treatment of the needle bearings. The preparation of the test samples and test conditions is presented in Table 5 below.

Table 5. Carbonitriding needle bearing test conditions.

Test Conditions	Rotation Speed (rpm)	Radial Load (kN)	Number of Bearings for Test (Pieces)	
			Conventional Heat Treatment	Carbonitriding Treatment
Normal load	4000	4.9	2	2
High load	4000	8.6	2	2

The most prevalent forms of wear in rolling bearings are surface fatigue wear, abrasive wear, and adhesive wear. Adhesive wear and fatigue wear occur when the conditions are inadequate to form the lubricant film required to separate the bearing's contacting surfaces.

The C/P values were 4.0 and 2.28, respectively, for the normal and high load conditions, with a viscosity ratio of k = 0.8. The experimental bearings exhibited high resistance to adhesive wear due to their elevated hardness, which was evidenced by the results of the conducted experiments. The low viscosity of the utilized lubricant may have resulted in the formation of slight adhesive wear between the contacting surfaces. It is possible that initial fatigue at the surface may result from surface defects caused by adhesive wear [25].

The standards used in this life test were the GB/T 6391-2010 [26] Rolling Bearings-Rated Dynamic Load and Rated Life and the GB/T 24607-2009 [27] Rolling Bearings-Life and Reliability Test and Evaluation.

4. Results

4.1. Effect of Carbonitriding Strengthening Treatment on Material Properties

4.1.1. Effect on Surface Hardness

The surface hardness of the conventionally heat-treated disc samples and carbonitriding-treated disc samples was evaluated using the HMV-G series micro-Vickers hardness tester. Five distinct positions on the surface of each test sample were selected for analysis, and the results are presented in Table 6.

Table 6. Comparison of samples' hardness.

	Treatment	HV1	HV2	HV3	HV4	HV5	Average
Hardness (HV)	General	757	788	757	757	804	772.6
	Carbonitriding	804	8740	780	884	865	841.4

The test results demonstrate that the average surface hardness of the carbonitriding treatment samples was significantly higher than that of the samples subjected to the conventional heat treatment, where the hardness value increased by 8.9%. It has been demonstrated that carbon and nitrogen co-infiltration heat treatment improves the nitrogen content of the surface material of AISI 52100 steel. The subsequent quenching and heat treatment of the samples resulted in the penetration of nitrogen atoms into the lattice of

the material. This caused the lattice to expand and distort, and increased the strength and hardness of the steel along with the increase in the nitrogen content [28]. Furthermore, the yield strength of the material was improved.

Equation (9) defines the linear relationship between the tensile strength and the hardness of a material. The Vickers hardness (HV) is converted into the Brinell hardness (HB) and then incorporated into Equation (9), calculating tensile strength σ_b.

$$\sigma_b = 237.9 + 1.394\text{HB} \tag{9}$$

The yield strength of the conventionally heat-treated sample was 2030 MPa, while the ultimate tensile strength was 2240 MPa in the life simulation. Table 6 demonstrates that the hardness of the surface of the needle bearings after the carbonitriding treatment was increased by 8.9%. Consequently, the yield strength of the carbonitriding-treated sample was 2210 Mpa, and the ultimate tensile strength was 2439 Mpa.

4.1.2. Effect on Residual Austenite

The diffraction peaks at (200) α, (200) γ, (211) α, (220) γ, and (311) γ were selected according to the XRD patterns. The residual austenite volume fraction was calculated using Equation (10):

$$V_\gamma = \frac{1}{n}\sum_{j=1}^{n}\frac{I_\gamma^j}{R_\gamma^j} \Big/ \left(\frac{1}{n}\sum_{j=1}^{n}\frac{I_\gamma^j}{R_\gamma^j} + \frac{1}{n}\sum_{j=1}^{n}\frac{I_\alpha^j}{R_\alpha^j}\right) \tag{10}$$

$$R = \frac{1}{V^2}F^2\rho\frac{1+\cos^2 2\theta}{\sin\theta \times \sin 2\theta}\exp(-2M) \tag{11}$$

where V_γ is the volume fraction (%) of the austenite phase; n is the number of diffraction peaks; R is the material scattering factor, which is calculated as shown in Equation (11); I is the integrated intensity of the diffraction peaks; θ is the diffraction angle; V is the volume of the single cell; F is the structure factor; ρ is the multiplicity factor; and exp(-2M) is the temperature factor.

Figure 5 illustrates the results of surface residual austenite detection in the conventionally heat-treated discs and carbonitriding-treated discs. The diffraction peaks of ferrite, indicated by (200) α and (211) α, and the diffraction peaks of austenite, indicated by (200) γ, (220) γ, and (311) γ, are shown. A comparison of Figure 5a,b reveals that the diffraction peak value of ferrite in the carbonitriding samples is significantly lower than that in the conventional samples, while the diffraction peak value of residual austenite is higher. This indicates that the residual austenite content of the sample is increased following the carbonitriding treatment. The residual austenite volume fractions of the conventionally heat-treated samples and the carbonitriding-treated samples calculated using Equation (10), were 7.37 $\pm$ 0.04% and 25.91 $\pm$ 0.12%, respectively. The residual austenite content increased by 251.58 $\pm$ 3.54%.

The greater the hardness of a material, the greater its resistance to wear indentation and the less likely it is to exhibit an indentation on the contact surface when contact is created. However, as the hardness of the material increases, its toughness is reduced, and its resistance to cracking is also reduced. Furthermore, an increase in the residual austenite content enhances the toughness of the material itself, which enhances the resistance to crack extension of the material. The carbonitriding treatment of materials resulted in the formation of nitrogen-containing martensite, which improved the hardness of the material's surface. This resulted in a comprehensive improvement in the material's wear resistance and resistance to damage. Consequently, the carbonitriding treatment of needle bearings effectively inhibited the generation and development of initial micro-cracks and improved the contact fatigue life of needle bearings.

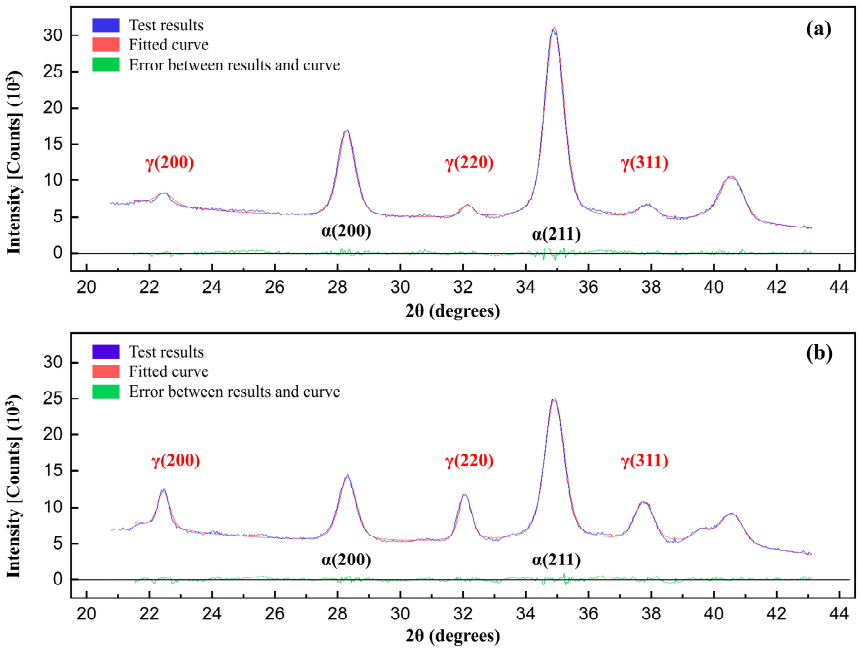

Figure 5. XRD diffraction intensity patterns of the samples: (**a**) conventional heat treatment sample; (**b**) carbonitriding treatment sample.

4.2. Effect of Carbon and Nitrogen Co-Infiltration Strengthening Methods on Microstructure

4.2.1. Before Friction Wear Test

Figure 6 shows the surface morphology and energy spectrum analysis of the conventionally heat-treated samples and carbonitriding-treated samples prior to the friction wear test. The EDS spectrum of randomly selected regions A and B are illustrated in Figure 6b,d. As depicted in Figure 6c, following the carbonitriding treatment, machining traces can still be observed on the surface of the test specimen. The surface morphology and the types and content of the constituent elements were nearly identical to those of the conventionally heat-treated specimen.

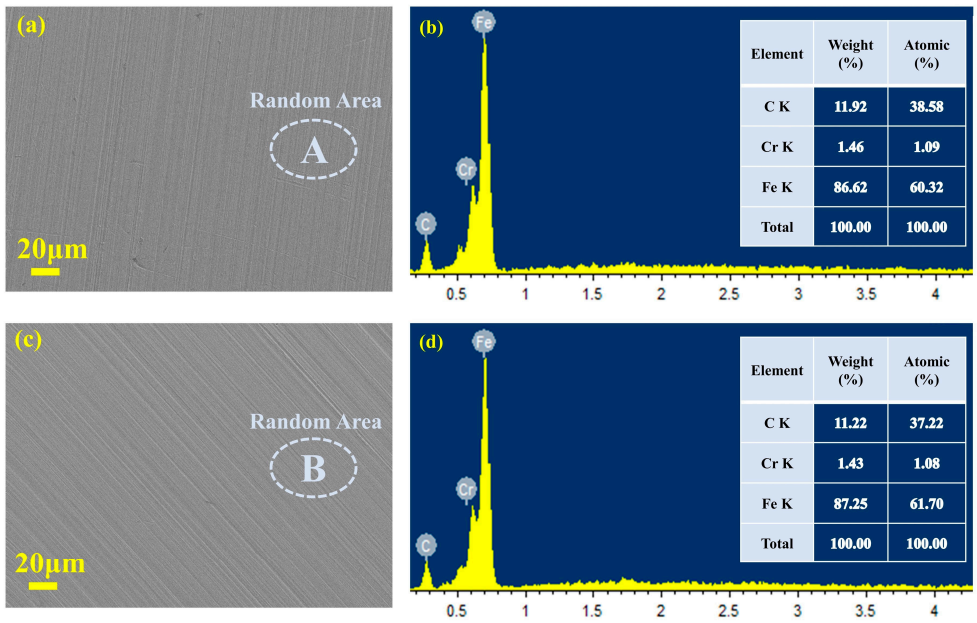

Figure 6. Surface morphology and energy spectrum analysis before the friction wear test: (**a**) SEM morphology of the conventionally heat-treated sample; (**b**) EDS spectrum of region A; (**c**) SEM morphology of the carbonitriding-treated sample; (**d**) EDS spectrum of region B.

4.2.2. After Friction Wear Test

Following the friction wear tests at 100 N and 200 N, the initial machining scratches were still visible on the surfaces of the conventionally heat-treated specimens, with only slight traces of the test wear being evident. After the friction and wear test at 300 N, the initial machining scratches disappeared, and were replaced by test scratches. Figure 7 illustrates the surface morphology and energy spectrum analysis results for the sample following the friction and wear tests at 100 N, 200 N, and 300 N loads, respectively. The EDS spectrum of randomly selected amplification regions A, B, and C are illustrated in Figure 7b,d,f.

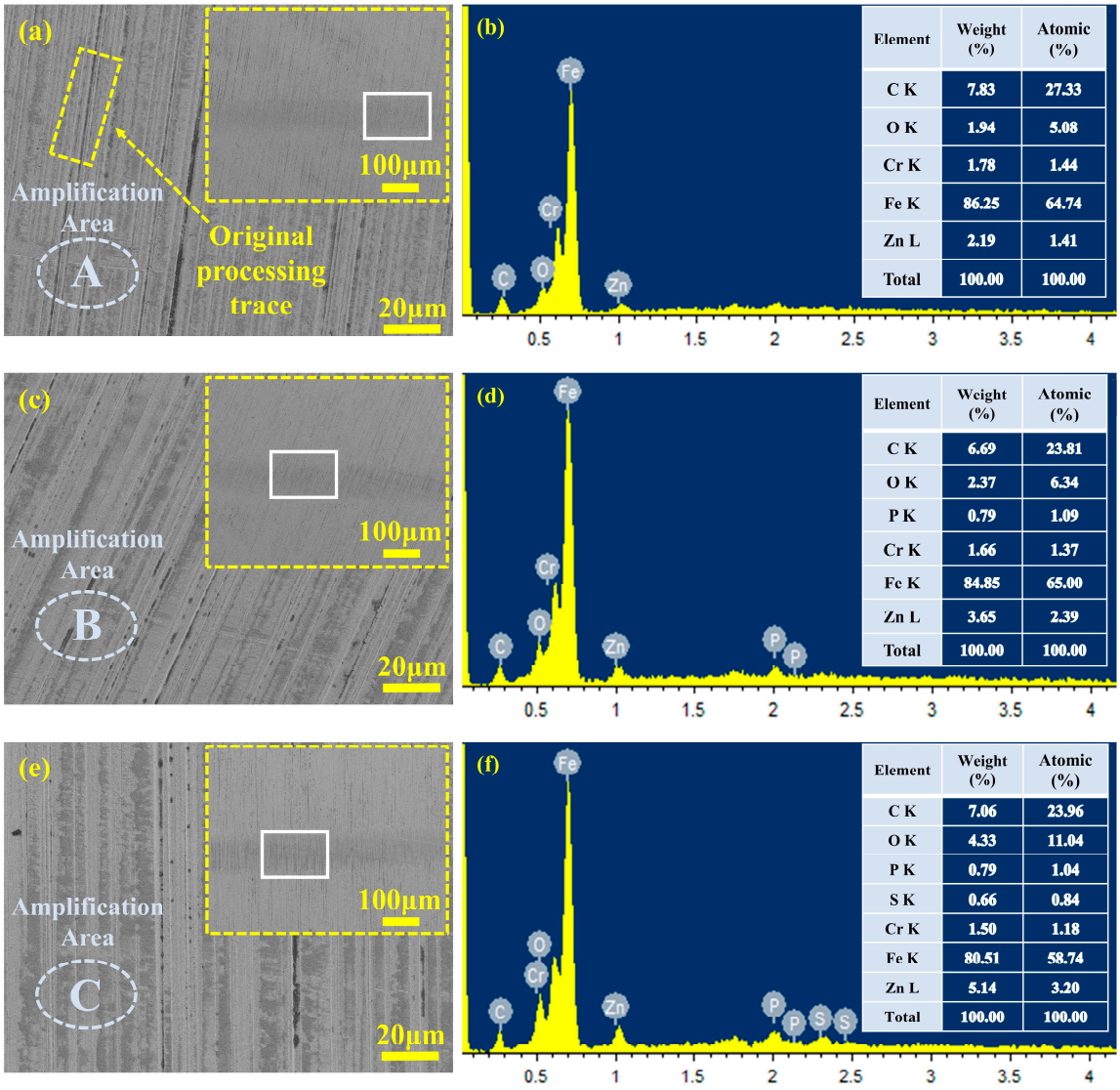

Figure 7. Surface morphology and energy spectrum analysis of the carbonitriding-treated samples after the friction wear test: (**a**) SEM morphology at 100 N; (**b**) EDS spectrum of region A; (**c**) SEM morphology at 200 N; (**d**) EDS spectrum of region B; (**e**) SEM morphology at 300 N; (**f**) EDS spectrum of region C.

Figure 7a demonstrates that after the 100 N friction and wear test, the surface of the sample exhibited only slight marks of movement, with the original scratches remaining intact. From Figure 7c,e, it can be observed that the surfaces of the carbonitriding-treated samples which were subjected to friction and wear tests at 200 N and 300 N loads did not exhibit significant friction and wear marks. Instead, the predominant scratches were those present prior to the tests. From Figure 7b,d,f, it can be observed that the surface element

composition and mass fraction of the carbonitriding-treated samples were comparable to those of the conventionally heat-treated samples.

The sample was subjected to a carbonitriding and quenching heat treatment, during which the nitrogen atoms formed a solid solution with the martensite matrix, thereby forming a nitrogen-containing martensite. The incorporation of nitrogen into the martensite matrix resulted in an effect similar to that of applying solid solution strengthening on the material. Concurrently, the dispersed carbon/nitrogen compounds on the martensitic matrix reinforced the bearing steel through the dispersion strengthening effect, and the comprehensive performance of the carbonitriding treatment enhanced the wear resistance of the material [13]. The above phenomenon demonstrates that the carbon and nitrogen co-infiltration treatment of the sample confers a certain degree of wear resistance, which effectively reduces the frictional wear of the bearings.

4.3. Effect of Carbonitriding Strengthening Method on Friction and Wear Performance

4.3.1. Effect on Coefficient of Friction

Figure 8a shows the coefficient of friction (COF) of the conventionally heat-treated samples under different loads with time. The first 300 s of the friction wear experiment constituted the break-in period, during which the COF varied greatly. After a sharp increase, the COF started to decrease and then entered a stabilization period, during which it slowly tended to stabilize. Under a load of 300 N, it was finally stabilized at 0.1499 ± 0.0004. Figure 8b depicts the time-dependent change curve of the COFs of the carbonitriding-treated samples under different loads. The COF was finally stabilized at 0.1454 ± 0.0002 under a load of 300 N. In comparison to the conventional samples, the COF of the carbonitriding-treated samples exhibited a notable decline under loads of 100 N and 200 N, with a more pronounced reduction observed under the load of 300 N. In comparison to the conventionally heat-treated samples, the reduction in the COF was more pronounced for the 100 N and 200 N test loads. Conversely, the reduction in the COF of the carbonitriding-treated samples was less pronounced at the 300 N load.

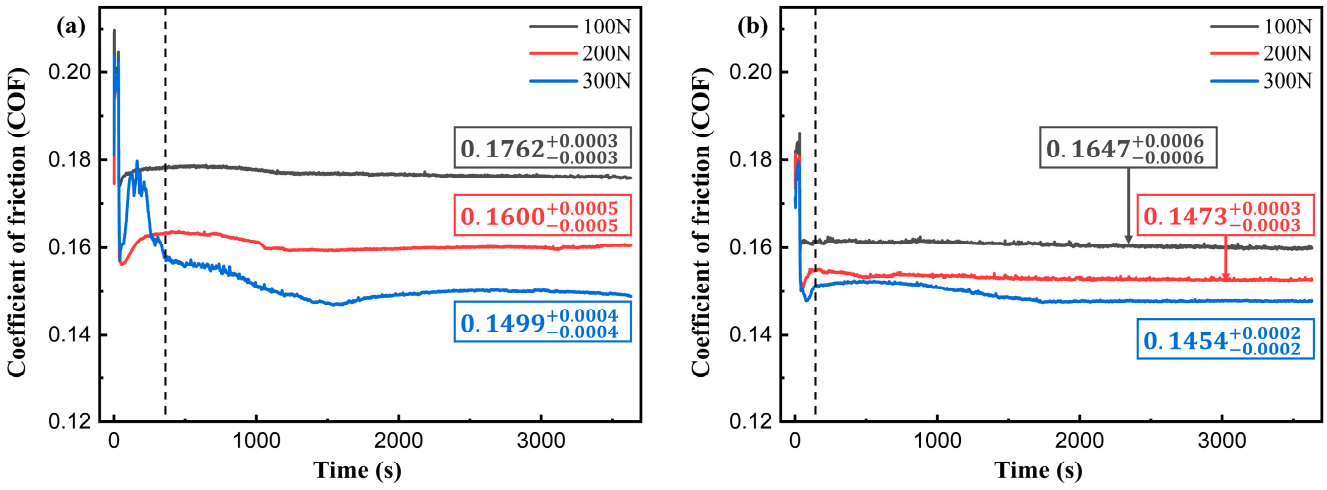

Figure 8. Coefficients of friction of samples: (**a**) conventionally heat-treated sample; (**b**) carbonitriding-treated sample.

4.3.2. Effect on Surface Wear Scar

Figure 9 compares the wear scar depths of the conventionally heat-treated samples. The depth of the conventionally heat-treated test samples after friction wear testing at a 100 N load was 0.176 μm. The wear scar depth in the friction wear test at a 300 N load was 0.623 μm, representing an increase of 0.447 μm, with a growth rate of 253.97%. A comparison of the depths of carbonitrided samples is presented in Figure 10. The wear scar depth of the test samples after the friction wear test at a 100 N load was 0.196 μm,

and the depth of the test samples after friction wear testing at a 300 N load was 0.253 µm, representing an increase of 0.057 µm or 29.08%.

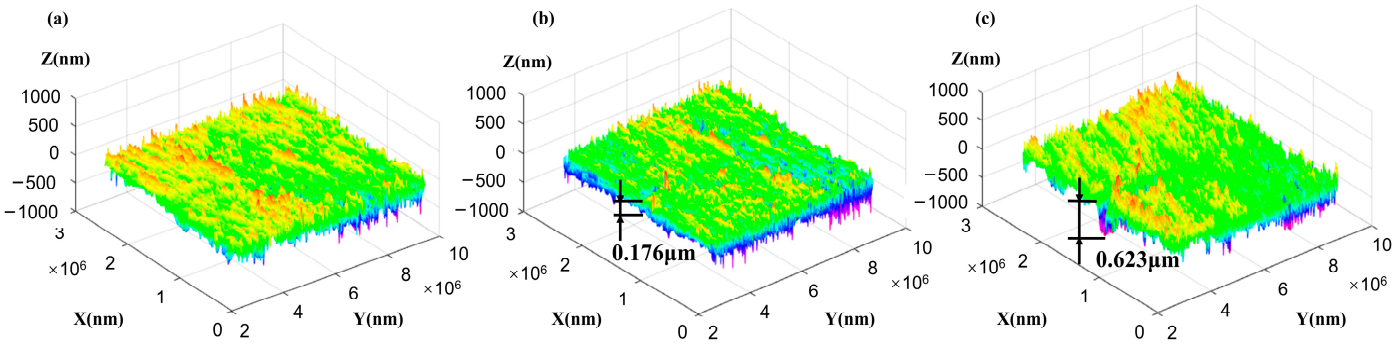

Figure 9. Comparison of the wear scar depths of conventionally heat-treated samples: (**a**) before the experiment; (**b**) under a load of 100 N; (**c**) under a load of 300 N.

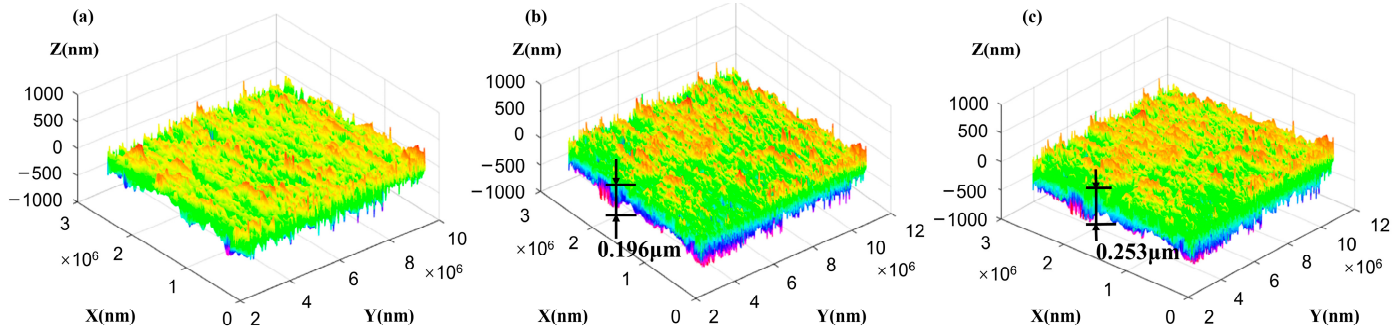

Figure 10. Comparison of the wear scar depths of carbonitriding-treated samples: (**a**) before the experiment; (**b**) under a load of 100N; (**c**) under a load of 300N.

4.3.3. Friction and Wear Performance Analysis

The presence of residual tensile stresses in the surface layers of needle bearing components has been demonstrated to reduce the performance and life of bearings [29]. The carbon and nitrogen co-infiltration treatment of the AISI 52100 bearing steel, whereby C and N atoms penetrate into the surface layer of the work piece, has been shown to effectively reduce the temperature of the onset of martensitic transformation. Concomitant with enhanced hardness in the infiltration layer, significant residual compressive stress is generated in the surface layer. Consequently, the strength and contact fatigue life of the bearing steel are enhanced.

Following the application of conventional heat treatment to a material, it becomes evident that the surface exhibits a notable degree of wear after undergoing a series of friction experiments. As the experiments progress, the original peaks of the surface become progressively worn down, either as wear chips or pressed into the surface. This results in a discernible alteration in the surface morphology and affects the values of the surface roughness and COF. As a consequence of the repeated application of alternating stresses between the contact surfaces, fatigue cracks gradually emerge at the surface or subsurface locations of the material and gradually expand into fatigue craters [30]. Due to the low surface hardness and toughness of conventionally heat-treated samples, fatigue cracks are readily produced and expand rapidly, resulting in localized furrow-like wear marks. The undulation of this surface varies significantly, as evidenced by the high growth rate of the wear marks and the high COF of the contact surface.

Following the carbonitriding treatment, the samples were subjected to a friction wear test, which revealed that the overall change to the surface was relatively minor. The initial roughness peak was flattened, the surface became flat, and the growth of the

wear marks was low. The surface pits exhibited no significant expansion and the furrow-like distribution on the surface was uniform and narrow in width. The above analysis demonstrates that carbonitriding can effectively enhance the wear resistance of the bearing steel and material surface.

4.4. Fatigue Life Analysis

4.4.1. Simulation Results

The requisite parameters were entered into Romax and the results of the damage simulation of the needle bearings were obtained, as shown in Table 7. In comparison to the fatigue damage of the conventionally heat-treated needle bearings, the fatigue damage rate of the needle bearings simulated under the ISO 281 [31] decreased by 3.3%. Furthermore, the fatigue damage rate calculated under the ISO/TS 16281 [32] decreased by 3.5%. The fatigue life simulated under the ISO 281 standard increased by 3.44%, while the fatigue life simulated under the ISO/TS 16281 standard increased by 3.79%.

Table 7. Needle bearing life simulation results.

Computational Item	Conventional	Carbonitriding
ISO 281 Damage (%)	33.4	32.3
ISO/TS 16281 Damage (%)	74.6	72.0
ISO 281 Lifetime (h)	1269.73	1313.43
ISO/TS 16281 Lifetime (h)	568.41	589.98

4.4.2. Test Results

A total of eight sets of bearings were prepared for the life comparison test of carbonitrided needle bearings. Four sets each of conventionally heat-treated and carbonitriding-treated needle bearings were subjected to normal-load and high-load tests. The fatigue life comparison results of the bearings subjected to conventional heat treatment and carbonitriding in normal load conditions are shown in Figure 11. The fatigue life of the bearings subjected to the different heat treatment processes was averaged, and it was determined that the fatigue life of carbonitrided needle bearings was increased by 384% and 463%, respectively, under normal-load conditions and high-load conditions. Additionally, the fatigue limit was increased by 31.9% under normal-load conditions and high-load conditions.

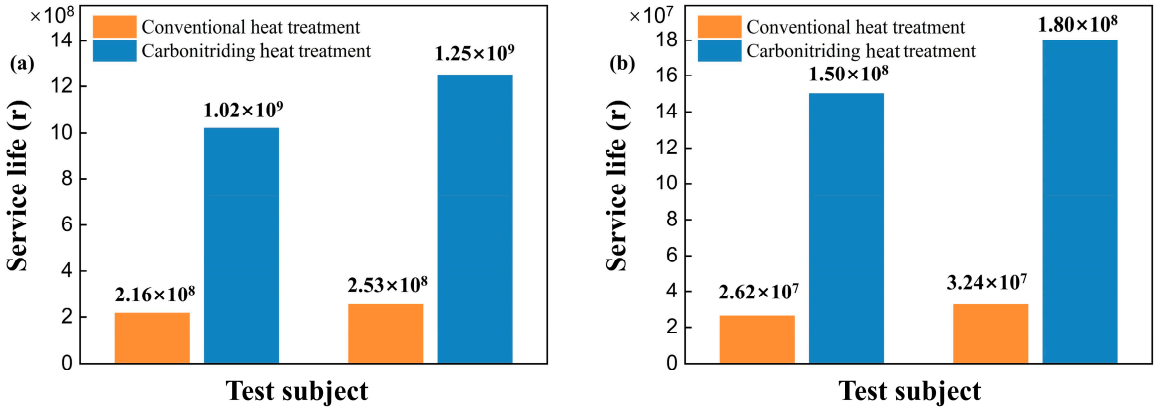

Figure 11. Service life of needle bearings: (**a**) normal-load conditions; (**b**) high-load conditions.

A conventionally heat-treated needle bearing and a carbonitriding-treated needle bearing were selected. The failure regions were observed using a magnifier, as shown in Figure 12.

When the needle bearing obtained by conventional heat treatment failed, it was observed that obvious contact fatigue pits appeared on the contact surface. The areas of the pits were smaller and the depths were larger, indicating that these positions were the

weak points of the material. This may be due to the residual compressive stress distribution being non-uniform or the hardness being lower. In the case of needle bearings subjected to carbonitriding heat treatment, the area of the failure region was larger, the number of pits was greater, and the depths were shallower when contact fatigue failure occurred. This phenomenon serves to illustrate that the surface residual stress distribution of needle bearings after carbonitriding treatment is more uniform, the comprehensive fatigue strength is improved, and the ability of each position to resist fatigue spalling is effectively enhanced.

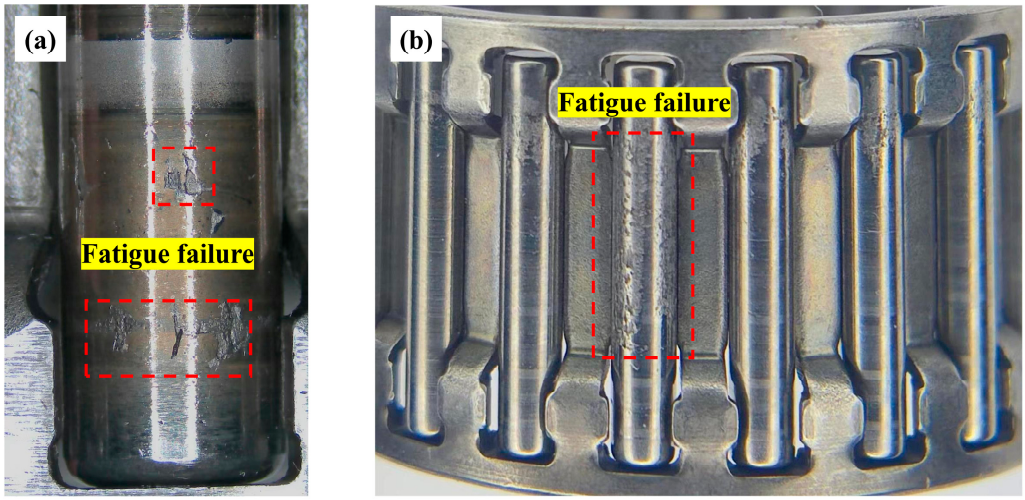

Figure 12. Needle bearing failure locations: (**a**) conventionally heat-treated needle roller; (**b**) carbonitrided needle roller.

5. Conclusions

In order to investigate the impact of carbonitriding surface strengthening treatment on the friction and wear performance and fatigue life of needle roller bearing surfaces, this study employed K28 × 33 × 19-type needle roller bearings for research. The principal findings are as follows:

1. After the carbonitriding treatment, the hardness of the AISI 52100 bearing samples increased by 8.9%, while the residual austenite content increased by 251.58 ± 3.54%. The enhancement in the fatigue characteristics of the bearing is a consequence of the combination of high surface hardness and residual austenite;
2. After performing the SRV friction and wear test, the surfaces of the conventionally heat-treated samples exhibited clear evidence of test wear, whereas the surfaces of the carbonitriding-treated samples did not. The surface scratches observed on the latter were primarily the initial scratches present prior to the test. The change in the surface COF of the carbonitriding samples was minimal, and the depth of the wear scar was significantly smaller than that of the conventionally heat-treated samples. This observation provides a clear indication of the impact of the carbonitriding treatment on the anti-wear performance;
3. The results of the test bench simulation indicate that the degree of damage due to fatigue to the bearings treated with carbonitriding was approximately 3.3% lower than that of a conventionally heat-treated bearing. Upon comparison with conventionally heat-treated bearings, the fatigue life of needle bearings that undergo carbonitriding was enhanced by 384% in the case of normal loads and by 463% in the context of high loads. Following the implementation of a uniform residual stress distribution on the carbonitrided bearing's surface, there was a notable enhancement in comprehensive fatigue strength. The capacity of each position to resist fatigue wear can also be observed.

Author Contributions: Conceptualization, Y.C.; methodology, Y.C.; software, X.P.; validation, X.P., L.H. and G.L.; formal analysis, L.L.; investigation, X.P., L.H., G.L. and L.L.; data curation, Y.C. and X.P.; writing—original draft preparation, X.P.; writing—review and editing, Y.C. and L.H.; visualization, G.L. and L.L.; funding acquisition, Y.C. All authors have read and agreed to the published version of the manuscript.

Funding: This research was funded by the Guangxi Key Research and Development Plan Special Project through grants No.2023AB07038.

Data Availability Statement: The data presented in this study are available upon request from the corresponding author.

Acknowledgments: Guangxi University and Hebei University of Technology are gratefully acknowledged for their support in producing the samples and providing technical services, respectively.

Conflicts of Interest: The authors declare no conflicts of interest.

References

1. Hao, L.J.; Chen, Y.; Li, G.X.; Zhang, M.; Wu, Y.M.; Liu, R.; Chen, G. Study on the Friction Characteristics and Fatigue Life of Manganese Phosphate Coating Bearings. *Lubricants* **2023**, *11*, 99. [CrossRef]
2. Schönbauer, B.M.; Mayer, H. Effect of small defects on the fatigue strength of martensitic stainless steels. *Int. J. Fatigue* **2019**, *127*, 362–375. [CrossRef]
3. Jouini, N.; Revel, P.; Thoquenne, G. Influence of surface integrity on fatigue life of bearing rings finished by precision hard turning and grinding. *J. Manuf. Processes* **2020**, *57*, 444–451. [CrossRef]
4. Azianou, A.E.; Debray, K.; Bolaers, F.; Chiozzi, P.; Palleschi, F. Fatigue behaviour FEM modeling of deep groove ball bearing mounted in automotive alternator submitted to variable loading. In Proceedings of the Conference on Fatigue Design and Material Defects, France, Paris, 11–13 June 2014.
5. Yessine, T.M.; Fabrice, B.; Fabien, B.; Sébastien, M. Study of ball bearing fatigue damage using vibration analysis: Application to thrust ball bearings. *Struct. Eng. Mech.* **2015**, *53*, 325–336. [CrossRef]
6. Wang, L.W.; Sheng, X.Y.; Luo, J.B. A peridynamic damage-cumulative model for rolling contact fatigue. *Theor. Appl. Fract. Mec.* **2022**, *121*, 103489. [CrossRef]
7. Morales-Espejel, G.E. Surface roughness effects in elastohydrodynamic lubrication: A review with contributions. *P. I. Mech. Eng. J-J. Eng.* **2014**, *228*, 1217–1242. [CrossRef]
8. Smolnicki, T.; Rusiński, E. Superelement-based modeling of load distribution in large-size slewing bearings. *J. Mech. Design* **2007**, *129*, 459–463. [CrossRef]
9. Lostado, R.; Martinez, R.F.; Mac Donald, B.J. Determination of the contact stresses in double-row tapered roller bearings using the finite element method, experimental analysis and analytical models. *J. Mech. Sci. Technol.* **2015**, *29*, 4645–4656. [CrossRef]
10. Kania, L. Modelling of rollers in calculation of slewing bearing with the use of finite elements. *Mech. Mach. Theory* **2006**, *41*, 1359–1376. [CrossRef]
11. Bakolas, V.; Roedel, P.; Koch, O.; Pausch, M. A first approximation of the global energy consumption of ball bearings. *Tribol T* **2021**, *64*, 883–890. [CrossRef]
12. Ilie, F. Diffusion and mass transfer mechanisms during frictional selective transfer. *Int. J. Heat Mass Tran.* **2018**, *116*, 1260–1265. [CrossRef]
13. Huan, Q.T.; Du, S.M.; Wang, M.D.; He, T.T.; Zhang, Y.Z. Effects of different chemical heat treatment on mechanical properties and tribological behavior of GCr15 steel. *Trans. Mater. Heat Treat.* **2021**, *42*, 117–123.
14. Wan, H.Y.; Lu, H.; Ren, Y.P.; Ma, C.; Chen, Y.; Xin, Z.D.; Cheng, L.; He, K.; Tu, X.C.; Han, Q. Strengthening mechanisms and tensile properties of 20Cr2Mn2Mo processed by laser shock peening and vacuum carbonitriding. *Surf. Coat. Tech.* **2022**, *439*, 128462. [CrossRef]
15. Rajan, K.; Joshi, V.; Ghosh, A. Effect of carbonitriding on endurance life of ball bearing produced from SAE 52100 bearing steels. *J. Surf. Eng. Mater. Adv. Technol.* **2013**, *3*, 172–177. [CrossRef]
16. Liu, M.D. Metallographic black microstructure analysis of GCr15 steel bearing rings after carbonitriding. *Heat Treat.* **2019**, *4*, 60–61.
17. Zhao, K.; Zhang, G.W.; Zhu, H.F. Effects of carbonitriding pretreatment on life of ball bearings. *Bearing* **2018**, *10*, 34–37.
18. Karamiş, M.B.; Odabaş, D. A simple approach to calculation of the sliding wear coefficient for medium carbon steels. *Wear* **1991**, *151*, 23–34. [CrossRef]
19. Kanchanomai, C.; Limtrakarn, W. Effect of residual stress on fatigue failure of carbonitrided low-carbon steel. *J. Mater. Eng. Perform.* **2008**, *17*, 879–887. [CrossRef]
20. Jiang, G.H.; Li, S.X.; Pu, J.B.; Wang, H.X.; Chen, Y.J. Rolling contact fatigue failure mechanism of martensitic bearing steel after carbonitriding. *China Surf. Eng.* **2022**, *35*, 12–23.
21. *ASTM A. 29/A 29M-04*; Standard Specification for Steel Bars, Carbon and Alloy, Hot-Wrought, General Requirements. ASTM International: West Conshohocken, PA, USA, 2017.

22. *ISO 683-17*; Heat-Treated Steels, Alloy Steels and Free-Cutting Steels—Part 17: Ball and Roller Bearing Steels. ISO: Geneva, Switzerland, 2023.
23. *ASTM D7421-11*; Standard Test Method for Determining Extreme Pressure Properties of Lubricating Oils Using High-Frequency, Linear-Oscillation (SRV) Test Machine. ASTM International: West Conshohocken, PA, USA, 2017.
24. Balarini, R.; Diniz, G.A.S.; Profito, F.J.; Souza, R.M. Comparison of unidirectional and reciprocating tribometers in tests with MoDTC-containing oils under boundary lubrication. *Tribol. Int.* **2020**, *149*, 105686. [CrossRef]
25. Vencl, A.; Gašić, V.; Stojanović, B. Fault tree analysis of most common rolling bearing tribological failures. *IOP Conf. Ser. Mater. Sci. Eng.* **2017**, *174*, 012048. [CrossRef]
26. *GB/T 6391-2011*; Rolling Bearings—Dynamic Load Ratings and Rating Life. Standardization Administration of China: Beijing, China, 2011.
27. *GB/T 24607-2009*; Rolling Bearings—Test and Assessment for Life and Reliability. Standardization Administration of China: Beijing, China, 2009.
28. Johnson, K.L. Failure atlas for Hertz contact machine elements. *Tribol. Int.* **1993**, *26*, 65–66. [CrossRef]
29. Zhai, Y.Z.; Xia, H.; Zhang, X.; Yang, X.L.; Wang, H.B.; Feng, J.H. Effect of nitrogen content on microstructure and mechanical properties of V-N microalloyed high strength steel bar. *Heat Treat. Met.* **2018**, *43*, 31–34.
30. Javadi, H.; Jomaa, W.; Texier, D.; Brochu, M.; Bocher, P. Surface roughness effects on the fatigue behavior of as-Machined Inconel718. *Solid State Phenom.* **2017**, *258*, 306–309.
31. *ISO 281: 2007*; Rolling Bearings—Dynamic Load Ratings and Rating Life. ASTM International: West Conshohocken, PA, USA, 2007.
32. *ISO/TS 16281*; Rolling Bearings—Methods for Calculating the Modified Reference Rating Life for Universally Loaded Bearings. ASTM International: West Conshohocken, PA, USA, 2008.